

Seismic evidence for a recently formed mantle upwelling beneath New England

Vadim Levin¹, Maureen D. Long², Peter Skryzalin¹, Yiran Li¹, and Ivette López²

¹Department of Earth and Planetary Sciences, Rutgers University, Piscataway, New Jersey 08854, USA

²Department of Geology and Geophysics, Yale University, New Haven, Connecticut 06511, USA

ABSTRACT

Lateral changes in seismic velocity 100–300 km beneath the Appalachian orogen (eastern North America) do not follow the pattern of its major terranes, suggesting that more recent, and possibly ongoing, geodynamic processes are taking place in the sub-lithospheric mantle. One prominent, sharply delineated, seismically slow feature underlying parts of New England (USA) likely reflects a volume of significantly elevated temperatures in the asthenosphere. Using numerous new observations of splitting in seismic shear waves from distant earthquakes, we show that this upper mantle volume also lacks the systematic directional dependence (anisotropy) of seismic wave speed that is ubiquitous beneath most of northeastern North America. This regional anisotropic fabric, which likely forms as the asthenosphere is sheared by North American plate motion, appears to be locally erased beneath central New England, with changes in its strength occurring over distances on the order of 50 km. Highly localized variation in the strength of seismic anisotropy in a region of strongly elevated asthenospheric temperature suggests the presence of a narrow thermal upwelling in the upper mantle beneath New England. The lack of obvious surface expressions (volcanism or uplift) and the small lateral scale of the hypothesized upwelling suggest a geologically recent phenomenon.

INTRODUCTION

The upper mantle beneath the Appalachian orogen in eastern North America contains a number of regions where seismic wave speed is significantly reduced relative to the regional mean (e.g., van der Lee and Nolet, 1997; Schmandt and Lin, 2014). These anomalies cut across the trend of the Appalachian terranes (Fig. 1) and thus likely post-date the Paleozoic assembly of Pangea, reflecting more recent (and possibly ongoing) geodynamic processes. The most prominent is the North Appalachian Anomaly (NAA) (e.g., Levin et al., 1995; Li et al., 2003) beneath New England and New York, USA (Fig. 1). Spatial association of reduced velocities in early models (van der Lee and Nolet, 1997; Menke and Levin, 2002) with the New England seamounts led to a proposed association of the NAA with the track of the Great Meteor hotspot beneath the North American continent (e.g., Eaton and Frederiksen, 2007).

More recent studies with improved lateral resolution afforded by EarthScope Transportable Array (TA) data (IRIS Transportable Array, 2003) identify a compact NAA that is largely limited to the volume east of the Appalachian front. In the model of Porter et al. (2016), the NAA has a shear wave velocity (V_s) of ~ 4.4 km/s, a 4% reduction relative to V_s beneath the craton (Fig. 1). Detailed images place the NAA mostly beneath the relatively thin lithosphere of the northern Appalachian orogen (e.g., Rychert et al., 2007). Using amplitudes of co-located anomalies in shear and compressional speed, Menke et al. (2016) affirmed that the NAA is a thermal feature, and estimated a $\sim 10\%$ reduction in V_s . Based on teleseismic body waves, the study of Menke et al. (2016) has good lateral resolution but lacks constraints on absolute velocities. Dong and Menke (2017) further showed that shear waves attenuate strongly within

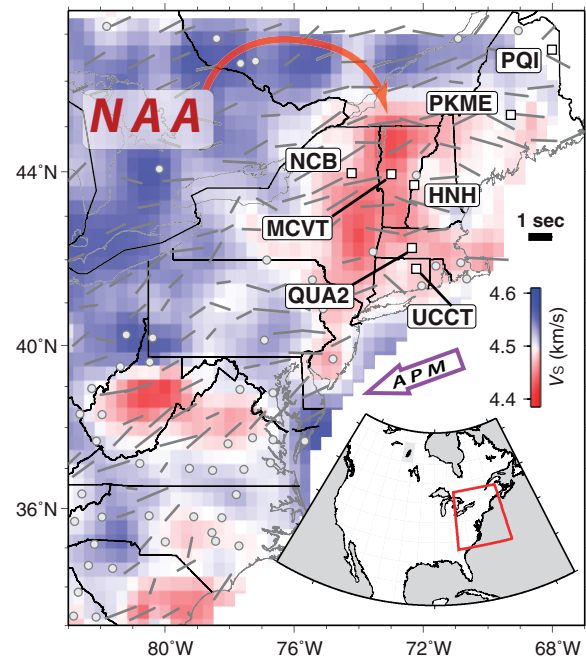


Figure 1. Shear wave speed (V_s) at 195 km depth (Porter et al., 2016) and anisotropy (Long et al., 2016) in eastern North America. Averaged shear wave splitting parameters are shown as bars aligned with fast polarization direction (ϕ) and scaled with time delay between fast and slow components (δt); scale bar in upper right. Sites with no splitting detected are shown as circles. Labeled boxes show locations of long-operating seismic observatories used for analysis of splitting intensity. Absolute plate motion (APM) direction (model HS3-NUVEL1A) is shown by open arrow. NAA—North Appalachian Anomaly.

the NAA, implying high temperature. Menke et al. (2016) explained the presence of an intense thermal anomaly in a region lacking active tectonics for ~ 100 m.y. by ongoing, localized mantle upwelling.

The intense, localized V_s perturbation represented by the NAA contrasts with existing constraints on the upper mantle fabric of the region, as expressed in observations of seismic anisotropy. Levin et al. (2000) used similarity of shear wave splitting patterns to argue for a regionally uniform anisotropic fabric composed of two layers corresponding to the lithosphere and the asthenosphere. Studies incorporating surface waves provided additional support for a multilayered model (e.g., Yuan et al., 2011). However, lateral resolution of anisotropy in these studies was not sufficient to detect changes on the scale of a few hundreds of kilometers. Recent comprehensive mapping of anisotropic properties using TA data by Long et al. (2016) and Yang et al. (2017) confirmed their general uniformity in a region that includes the NAA, with a certain degree of local variation. One notable outlier was an absence of measurable splitting at site I61A on the border between New Hampshire and Vermont, while locations

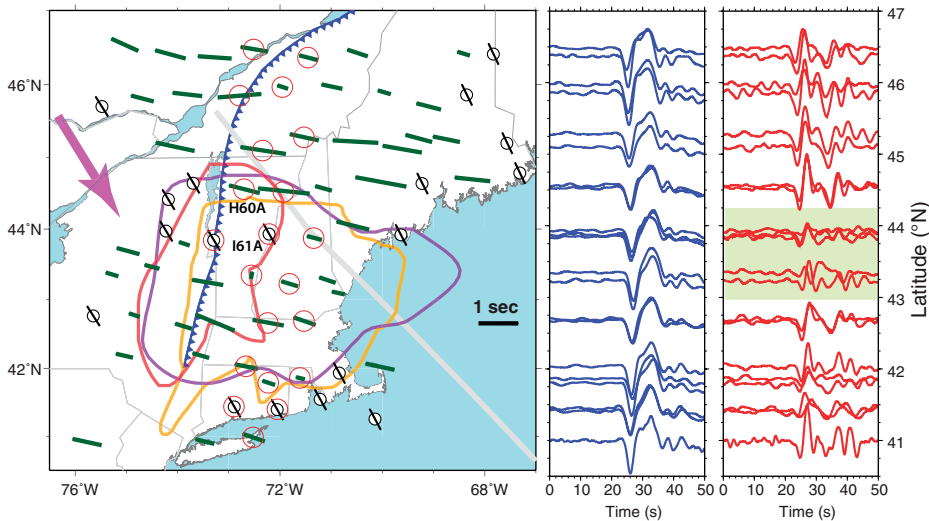


Figure 2. An SKS phase observed throughout New England (USA) region. Left: Shear wave splitting measurements shown by green bars aligned with fast polarization direction (ϕ) and scaled by time delay between fast and slow components (δt). Black circles are NULL measurements, with thin black bars aligned to wave propagation direction (magenta arrow). Sites mentioned in text are labeled. Outlines of North Appalachian Anomaly (NAA): purple—3% below mean shear wave velocity (V_s) in Schmandt and Lin (2014); red—4.45 km/s contour in Porter et al. (2016); yellow—0.06 km/s below mean V_s in Menke et al. (2016). Blue line with teeth denotes Appalachian front; thick gray line is track of Great Meteor hotspot. Right: Record section of selected sites (red circles in map) within an ~100-km-wide north-south swath. Reduced transverse amplitude is seen at sites between 43°N and 44°N (green background in shear wave record, right panel), consistent with small or NULL splitting within NAA.

within ~100 km of it yielded clear evidence for significant splitting (Long et al., 2016; Figs. 1 and 2). Significantly, the site with no observed splitting lies within the NAA, above the local disruption of upper mantle flow via upwelling proposed by Menke et al. (2016). Similarly, Yang et al. (2017) documented a modest reduction in splitting delay times at TA stations in New England. However, the short duration of the TA deployment makes the robustness of these observations difficult to evaluate.

Here we present observations of shear wave splitting from a set of long-running observatories not included in either the work of Levin et al. (2000) or the recent survey by Long et al. (2016). Our results demonstrate that splitting of core-refracted shear waves within the outline of the NAA is significantly weaker than at comparable locations toward its edges and beyond them. This splitting reduction is consistent with a localized change in anisotropic fabric that would be expected in a case of subvertical flow overprinting the broadly uniform upper mantle fabric detected throughout the region. Our findings bolster the hypothesis that the NAA corresponds to an upward limb of the small-scale convection cell formed at the edge of the thick cratonic lithosphere to the west (Menke et al., 2016).

DATA AND METHODS

Our data come from permanent and temporary broadband seismic observatories in the region (Table DR1 in the GSA Data Repository¹; Figs. 1 and 2). Stations operating for a decade or more (Fig. 1) are particularly crucial for our analysis, as many years of data are commonly required to capture the details of splitting behavior (e.g., Long and van der Hilst, 2005). We use records of core-refracted shear waves (SKS, SKKS, PKS; collectively denoted XKS), seeking to evaluate the degree of birefringence in their particle motion arising from their propagation through anisotropic materials of the upper mantle (Vinnik et al., 1984). XKS phases are initially radially polarized (within the vertical plane containing source and receiver). Deviation from this indicates birefringence (splitting) and reflects the influence of anisotropic upper mantle beneath the station (Savage, 1999).

Following Long and van der Hilst (2005), we estimate shear wave splitting using three techniques and compare their outcomes to assess the degree of complexity in the anisotropic structure at depth. Specifically, we employ the rotation-correlation method (RC; Ando et al., 1983), the minimum energy method (SC; Silver and Chan, 1991), and the splitting intensity technique (SI; Chevrot, 2000). A brief summary of the methods

is provided in the Data Repository, and a detailed treatment may be found in Long and van der Hilst (2005). All three methods are implemented in the SplitLab analysis package (Wüstefeld et al., 2008) modified to include the SI technique (Deng et al., 2017).

RESULTS

Figure 2 shows regional variation in the waveforms and the splitting parameters obtained using an SKS phase from a 30 May 2015 earthquake near the Bonin Islands, Japan (magnitude $M_w=7.8$, depth 664 km). Fast polarizations (ϕ) are very similar throughout the region, with two coherent groups of NULL (no splitting) measurements: one near the Atlantic coast around Cape Cod (Massachusetts), and another around the southern part of Lake Champlain (Vermont and New York). This event was not included in the analysis of Long et al. (2016); thus, it is encouraging that it replicates their observation of weak or absent splitting within the NAA.

We carried out a systematic estimation of shear wave splitting at seven long-running sites (Fig. 1), some (sites MCVT, HNH, QUA2) within the outlines of the NAA, and others (sites PQI, PKME, NCB, UCCT) outside of it or near its border. XKS phases from earthquakes with $M_w > 6$ at distances of 85°–180° were visually inspected and chosen for analysis on the basis of record clarity, separation from other phases present in the seismogram, and backazimuthal coverage. In assembling the data set, we emphasized directional coverage, thus events from less populated directions were given more attention in the selection process. Table DR2 lists station information and observation characteristics.

For every phase chosen, we measured birefringence using the methods discussed above. Figure DR1 in the Data Repository illustrates cases of high-quality splitting and NULL measurements. Altogether, we produced 622 measurements, of which 253 (~40%) were NULLs. The fraction of NULL measurements varied markedly among sites, from as low as 23% (site UCCT) to as high as 72% (site HNH). All measurements are shown in Table DR3. Figure DR2 shows stereoplots of all measurements for the seven sites, illustrating general patterns of splitting measurements and NULL results.

Figure 3 presents SI measurements as a function of backazimuth for sites HNH (within the NAA) and NCB (on its western edge). SI values are expected to form quasi-sinusoidal patterns. For comparison, we predict SI values using the formulation proposed by Chevrot (2000):

$$SI = \delta t \times \sin[2(\phi_0 - \phi)], \quad (1)$$

where δt is the time delay between fast and slow components, ϕ_0 is backazimuth, and ϕ is the fast polarization direction. For this prediction, we use average δt and ϕ values for each site from the RC method (not including NULL measurements), and we also obtain best-fitting values for (ϕ , δt)

¹GSA Data Repository item 2018020, details on data sources, analysis methods, and results of shear wave splitting measurements, including Figures DR1 and DR2, and Tables DR1–DR3, is available online at <http://www.geosociety.org/datarepository/2018/> or on request from editing@geosociety.org.

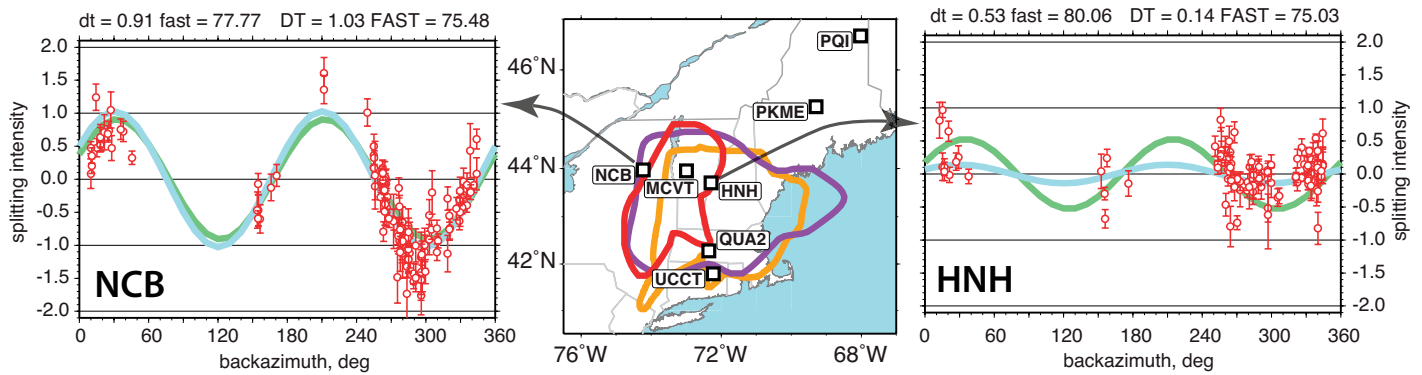


Figure 3. Splitting intensity (red circles with error bars) measurements for two sites plotted over best-fitting sinusoidal functions (blue) and predictions based on average splitting parameters (green). DT/dt—best fitting / average delay in sec; FAST/fast—best-fitting / average fast polarization in degrees clockwise from north. North Appalachian Anomaly (NAA) outlines are as in Figure 2.

via a nonlinear least-squares fit of the SI data with a function of the form $a \times \sin[2(\phi_0 - \phi)]$. At all sites except HNH, the values of δt and ϕ obtained via these two different ways are very close (see Fig. DR3).

Figure 3 and Figures DR2 and DR3 demonstrate a marked difference in the strength of shear wave birefringence observed within the NAA and outside of it. Interior stations (HNH, MCVT, QUA2) exhibit much weaker splitting using all three methods. Thus our results, based on data from long-running stations heretofore not examined in a systematic way, confirm the existence of a localized disruption of the seismic anisotropy signal registered by near-vertically propagating shear waves in an area spatially coincident with the NAA.

DISCUSSION

XKS phases integrate the anisotropic signal along the entire near-vertical receiver-side path through the upper mantle. To evaluate the vertical distribution of the anisotropic material, we rely on considerations of the Fresnel zone size, a wavelength-specific estimate of the width of the anisotropic volume contributing to the measurement (e.g., Salimbeni et al., 2008). When nearby sites display different splitting signals for the same phase (Fig. 2), the cause of the difference has to reside in a region where the ray paths of the corresponding waves diverge enough for the Fresnel zones to separate. Using a relationship:

$$R_f = 0.5\sqrt{T \times V \times h}, \quad (2)$$

where R_f is the radius of the Fresnel zone, T is the period, V is the velocity, and h is depth (Salimbeni et al., 2008), we obtain R_f values of 24 (34) km for $T = 5$ s, $V = 4.5$ km/s, and $h = 100$ (200) km. Similarly, from finite-difference calculations of upgoing shear waves, Rumpker and Ryberg (2000) estimated the width of a “transitional” region between two clearly distinct splitting measurements to be ~ 55 (75) km for period $T = 4$ s (see the Data Repository, section 4). Given the 70–80 km separation between TA sites in the region (e.g., sites H60A and I61A in Fig. 2), abrupt lateral changes in the upper 200 km beneath the surface will be resolvable.

Average ϕ values estimated at all seven long-operating sites are very similar (Table DR2 and Fig. DR3). This orientation ($\sim 80^\circ$ NE) is reasonably close to the absolute plate motion (APM) estimated in the hotspot reference frame ($\sim 250^\circ$ SE for model HS3-NUVEL1A; Gripp and Gordon, 2002; see Fig. 1), suggesting that sub-lithospheric shear is the major cause of the observed splitting. Under this assumption, average δt at individual sites provides an estimate of the vertical extent of the coherently sheared region in the asthenosphere using a relationship:

$$L = \delta t \ V / A, \quad (3)$$

where L is thickness, V is velocity, and A is anisotropy percentage (Helffrich, 1995). Assuming $A = 4\%$ and $V = 4.5$ km/s, and using δt values from the fit to the SI values (Table DR2), we obtain a range of L values from ~ 16 km to ~ 130 km. Conversely, fixing the thickness L at 100 km, we can evaluate

A , obtaining values between 0.6% and 5%. Both estimates suggest that the asthenospheric upper mantle beneath the NAA, particularly beneath station HNH, has a substantially weaker signature of the subhorizontal rock fabric relative to that present elsewhere in the region. This suggests, in turn, a localized perturbation to mantle flow.

Such a model provides a straightforward explanation for both the anisotropic signal and the low isotropic velocities observed in the tomography; however, we cannot totally rule out other causes for the local change in δt . A localized perturbation in lithospheric anisotropy oriented favorably to cancel the mantle flow signal could lead to a reduction in δt values. Diagnosing multiple layers of anisotropy with the SI technique is difficult because a sinusoidal pattern of values is expected in all cases (Long and van der Hilst, 2005). With two layers of anisotropy (e.g., Levin et al., 2000), individual XKS phases should yield large δt values when they travel along anisotropy axes in either the lithosphere or the asthenosphere. In contrast, we see an omnidirectional reduction of δt within the NAA. Contributions to splitting from anisotropy within the lowermost mantle may be diagnosed by differences in splitting parameters for SKS and SKKS phases for the same event-station pairs (e.g., Deng et al., 2017). We expect such contributions to be small and limited to narrow backazimuthal ranges, as only a few such pairs in our data set exhibit discrepancies (Table DR4).

With lithospheric overprint requiring a particular arrangement of its fabric, and lacking evidence that the lowermost mantle makes a major contribution to our observations, we favor a perturbation in the upper mantle flow field as the cause for the reduction in δt . Based on this finding, and on evidence for the thermal character of the NAA (Menke et al., 2016; Dong and Menke, 2017), we propose a conceptual model of localized disruption to the background asthenospheric mantle flow dominated by plate motion–parallel shear (Fig. 4). This upward flow beneath central New England overprints the preexisting olivine crystallographic preferred orientation (CPO), causing a rotation of the olivine fast axes to a more vertical orientation and weakening the anisotropic signal experienced by XKS waves (which are sensitive to azimuthal variations in V_s in the horizontal plane). We propose that this local upwelling represents the return flow associated with a convection cell at the edge of the thick cratonic lithosphere to the west (cf. King and Anderson, 1998; Menke et al., 2016). Similar vertical mantle flow associated with a downward limb of an edge-driven convection cell has previously been invoked to explain weak or absent SKS splitting beneath the southeastern USA (Long et al., 2010). In both cases, the location of near-vertical flow is controlled by the preexisting lithospheric structure of the North American continent. An alternative scenario of an upwelling originating in the deep mantle is unlikely, as there is no clear evidence from global mantle tomography for such a feature (e.g., Ritsema et al., 2011).

The lack of surface expression in either topography or gravity above the proposed upwelling may be attributed to the small effect it would have on

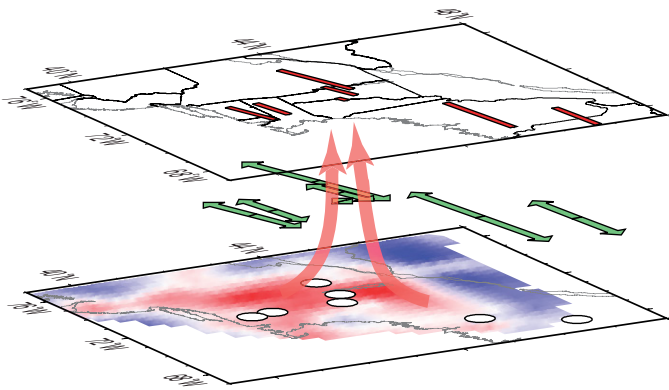


Figure 4. Splitting parameters obtained by fitting $\sin(2\phi)$ patterns (where ϕ is fast polarization direction) to splitting intensity technique (SI) values (Table DR1 [see footnote 1]) are plotted as red bars centered at observing sites (white circles), aligned with fast orientations, and scaled with delays. Scaled versions of same parameters shown as two-headed green arrows represent relative strength of azimuthal anisotropy in asthenosphere. Upward arrows in region where we infer very weak azimuthal anisotropy represent proposed asthenospheric upwelling within North Appalachian Anomaly.

an elastically thick North American plate due to its small lateral scale (~50 km diameter) and the relatively weak expected buoyancy. As hot mantle upwellings lose much of their thermal signature in ~60 m.y. (e.g., Eaton and Fredericksen, 2007), the presence of the NAA in the upper mantle implies its geologically recent formation. Similarly, the lack of heat flow or volcanic anomalies above it suggest that this feature is relatively recent (tens of millions of years old), and that any excess heat delivered to the base of the lithosphere has not had time to reach the surface via conduction.

ACKNOWLEDGMENTS

This work was supported by the EarthScope program via grants EAR-1147831 (Rutgers University) and EAR-1251515 (Yale University). Archives and science support tools of the Incorporated Research Institutions for Seismology (IRIS) Data Management Center were used to select and extract data. Helpful reviews by David Snyder and two anonymous reviewers are gratefully acknowledged. Figures were drafted using Generic Mapping Tools (GMT) (Wessel and Smith, 1995).

REFERENCES CITED

Ando, M., Ishikawa, Y., and Yamazaki, F., 1983, Shear wave polarization anisotropy in the upper mantle beneath Honshu, Japan: *Journal of Geophysical Research*, v. 88, p. 5850–5864, <https://doi.org/10.1029/JB088iB07p05850>.

Chevrot, S., 2000, Multichannel analysis of shear wave splitting: *Journal of Geophysical Research*, v. 105, p. 21,579–21,590, <https://doi.org/10.1029/2000JB900199>.

Deng, J., Long, M.D., Creasy, N., Wagner, L., Beck, S., Zandt, G., Tavera, H., and Minaya, E., 2017, Lowermost mantle anisotropy near the eastern edge of the Pacific LLSVP: Constraints from SKS-SKKS splitting intensity measurements: *Geophysical Journal International*, v. 210, p. 774–786, <https://doi.org/10.1093/gji/ggx190>.

Dong, M.T., and Menke, W.H., 2017, Seismic high attenuation region observed beneath southern New England from teleseismic body wave spectra: Evidence for high asthenospheric temperature without melt. *Geophysical Research Letters*, v. 44, <https://doi.org/10.1002/2017GL074953> (in press).

Eaton, D.W., and Fredericksen, A., 2007, Seismic evidence for convection-driven motion of the North American plate: *Nature*, v. 446, p. 428–431, <https://doi.org/10.1038/nature05675>.

Gripp, A.E., and Gordon, R.G., 2002, Young tracks of hotspots and current plate velocities: *Geophysical Journal International*, v. 150, p. 321–361, <https://doi.org/10.1046/j.1365-246X.2002.01627.x>.

Helfrich, G., 1995, Lithospheric deformation inferred from teleseismic shear wave splitting observations in the United Kingdom: *Journal of Geophysical Research*, v. 100, p. 18,195–18,204, <https://doi.org/10.1029/95JB01572>.

IRIS (Incorporated Research Institutions for Seismology) Transportable Array, 2003, USArray Transportable Array: International Federation of Digital Seismograph Networks, Other/Seismic Network, <https://doi.org/10.7914/SN/TA>.

King, S.D., and Anderson, D.L., 1998, Edge-driven convection: Earth and Planetary Science Letters, v. 160, p. 289–296, [https://doi.org/10.1016/S0012-821X\(98\)00089-2](https://doi.org/10.1016/S0012-821X(98)00089-2).

Levin, V., Lerner-Lam, A., and Menke, W., 1995, Anomalous mantle structure at the Proterozoic-Paleozoic boundary in northeastern US: *Geophysical Research Letters*, v. 22, p. 121–124, <https://doi.org/10.1029/94GL02693>.

Levin, V., Park, J., Brandon, M.T., and Menke, W., 2000, Thinning of the upper mantle during the late Paleozoic Appalachian orogenesis: *Geology*, v. 28, p. 239–242, [https://doi.org/10.1130/0091-7613\(2000\)28<239:TOTUMD>2.0.CO;2](https://doi.org/10.1130/0091-7613(2000)28<239:TOTUMD>2.0.CO;2).

Li, A., Forsyth, D.W., and Fischer, K.M., 2003, Shear velocity structure and azimuthal anisotropy beneath eastern North America from Rayleigh wave inversion: *Journal of Geophysical Research*, v. 108, 2362, <https://doi.org/10.1029/2002JB002259>.

Long, M.D., and van der Hilst, R.D., 2005, Estimating shear-wave splitting parameters from broadband recordings in Japan: A comparison of three methods: *Bulletin of the Seismological Society of America*, v. 95, p. 1346–1358, <https://doi.org/10.1785/0120040107>.

Long, M.D., Benoit, M.H., Chapman, M.C., and King, S.D., 2010, Upper mantle anisotropy and transition zone thickness beneath southeastern North America and implications for mantle dynamics: *Geochemistry Geophysics Geosystems*, v. 11, Q10012, <https://doi.org/10.1029/2010GC003247>.

Long, M.D., Jackson, K.G., and McNamara, J.F., 2016, SKS splitting beneath Transportable Array stations in eastern North America and the signature of past lithospheric deformation: *Geochemistry Geophysics Geosystems*, v. 17, p. 2–15, <https://doi.org/10.1002/2015GC006088>.

Menke, W., and Levin, V., 2002, Anomalous seaward dip of the lithosphere-asthenosphere boundary beneath northeastern US detected using differential-array measurements of Rayleigh waves: *Geophysical Journal International*, v. 149, p. 413–421, <https://doi.org/10.1046/j.1365-246X.2002.01652.x>.

Menke, W., Skryzalin, P., Levin, V., Harper, T., Darbyshire, F., and Dong, T., 2016, The Northern Appalachian Anomaly: A modern asthenospheric upwelling: *Geophysical Research Letters*, v. 43, p. 10,173–10,179, <https://doi.org/10.1002/2016GL070918>.

Porter, R., Liu, Y., and Holt, W.E., 2016, Lithospheric records of orogeny within the continental U.S.: *Geophysical Research Letters*, v. 43, p. 144–153, <https://doi.org/10.1002/2015GL066950>.

Ritsema, J., van Heijst, H.J., Deuss, A., and Woodhouse, J.H., 2011, S40RTS: A degree-40 shear-velocity model for the mantle from new Rayleigh wave dispersion, teleseismic traveltimes, and normal-mode splitting function measurements: *Geophysical Journal International*, v. 184, p. 1223–1236, <https://doi.org/10.1111/j.1365-246X.2010.04884.x>.

Rümpker, G., and Ryberg, T., 2000, New “Fresnel-zone” estimates for shear-wave splitting observations from finite-difference modeling: *Geophysical Research Letters*, v. 27, p. 2005–2008, <https://doi.org/10.1029/2000GL01423>.

Rychert, C.A., Rondenay, S., and Fischer, K.M., 2007, P-to-S and S-to-P imaging of a sharp lithosphere-asthenosphere boundary beneath eastern North America: *Journal of Geophysical Research*, v. 112, B08314, <https://doi.org/10.1029/2006JB004619>.

Salimbeni, S., Pondrelli, S., Margheriti, L., Park, J., and Levin, V., 2008, SKS splitting measurements beneath the Northern Apennines region: A case of oblique trench retreat: *Tectonophysics*, v. 462, p. 68–82, <https://doi.org/10.1016/j.tecto.2007.11.075>.

Savage, M.K., 1999, Seismic anisotropy and mantle deformation: What have we learned from shear wave splitting?: *Reviews of Geophysics*, v. 37, p. 65–106, <https://doi.org/10.1029/98RG02075>.

Schmandt, B., and Lin, F.-C., 2014, P and S wave tomography of the mantle beneath the United States: *Geophysical Research Letters*, v. 41, p. 6342–6349, <https://doi.org/10.1002/2014GL061231>.

Silver, P.G., and Chan, W.W., 1991, Shear wave splitting and subcontinental mantle deformation: *Journal of Geophysical Research*, v. 96, p. 16,429–16,453, <https://doi.org/10.1029/91JB00899>.

van der Lee, S., and Nolet, G., 1997, Upper mantle S velocity structure of North America: *Journal of Geophysical Research*, v. 102, p. 22,815–22,838, <https://doi.org/10.1029/97JfB01168>.

Vinnik, L.P., Kosarev, G.L., and Makeyeva, L.I., 1984, Anisotropy of the lithosphere from the observations of SKS and SKKS phases: *Doklady Akademii Nauk SSSR*, v. 278, p. 1335–1339 [in Russian].

Wessel, P., and Smith, W.H.F., 1995, New version of the Generic Mapping Tools released: *Eos (Transactions, American Geophysical Union)*, v. 76, p. 329.

Wüstefeld, A., Bokelmann, G.H.R., Zaroli, C., and Barruol, G., 2008, SplitLab: A shear-wave splitting environment in Matlab: *Computers & Geosciences*, v. 34, p. 515–528, <https://doi.org/10.1016/j.cageo.2007.08.002>.

Yang, B.B., Liu, Y., Dahm, H., Liu, K.H., and Gao, S.S., 2017, Seismic azimuthal anisotropy beneath the eastern United States and its geodynamic implications: *Geophysical Research Letters*, v. 44, p. 2670–2678, <https://doi.org/10.1002/2016GL071227>.

Yuan, H., Romanowicz, B., Fischer, K.M., and Abt, D., 2011, 3-D shear wave radially and azimuthally anisotropic velocity model of the North American upper mantle: *Geophysical Journal International*, v. 184, p. 1237–1260, <https://doi.org/10.1111/j.1365-246X.2010.04901.x>.

Manuscript received 18 August 2017

Revised manuscript received 25 October 2017

Manuscript accepted 27 October 2017

Printed in USA